Hấp phụ Asen hiệu quả bằng vật liệu vỏ sò biến tính phosphate thân thiện môi trường

TÓM TẮT

Ô nhiễm asen trong các hệ thống nước, đặc biệt là từ nguồn nước thải mỏ axit (acid mine drainage), gây ra những rủi ro nghiêm trọng đối với môi trường và sức khỏe con người do độc tính và khả năng di động cao của arsenat (As(V)). Trong nghiên cứu này, vỏ sò được tái sử dụng và chuyển hóa thành vật liệu vỏ sò biến tính phosphate (PMOS) như một chất hấp phụ thân thiện với môi trường và có chi phí thấp để loại bỏ As(V). PMOS được chế tạo thông qua quá trình xử lý nhiệt-hóa học kết hợp với giai đoạn biến tính phosphate, và đặc tính hấp phụ của vật liệu được khảo sát có hệ thống dưới các điều kiện khác nhau. Kết quả cho thấy hiệu suất loại bỏ As(V) phụ thuộc mạnh vào pH, thời gian tiếp xúc, nồng độ ban đầu và liều lượng chất hấp phụ; hiệu suất tối ưu (~95%) đạt được trong khoảng pH từ 3 đến 7, với liều lượng 1,0 ÷ 1,5 g/L và đạt trạng thái cân bằng sau 100 phút. Phân tích động học xác nhận rằng quá trình hấp phụ tuân theo mô hình giả bậc hai (pseudo-second-order), cho thấy cơ chế hấp phụ hóa học chiếm ưu thế, trong khi các nghiên cứu đẳng nhiệt cho thấy mô hình Freundlich phù hợp nhất, với dung lượng hấp phụ cực đại đạt 46,34 mg/g. Kết quả đặc trưng cấu trúc xác nhận sự gắn kết thành công của các nhóm phosphate, giúp tăng cường ái lực đối với arsenat thông qua tương tác tĩnh điện, trao đổi ion và tạo phức bề mặt. Đáng chú ý, các thử nghiệm tái sử dụng cho thấy PMOS vẫn duy trì hơn 80% hiệu suất loại bỏ sau năm chu kỳ hấp phụ-giải hấp, chứng minh độ bền tái sinh tốt của vật liệu. Những phát hiện này cho thấy PMOS là vật liệu tiềm năng, bền vững và kinh tế cho quá trình xử lý asen trong nước bị ảnh hưởng bởi nước thải mỏ axit, đồng thời góp phần thúc đẩy chiến lược kinh tế tuần hoàn thông qua việc tái giá trị hóa chất thải nuôi trồng thủy sản.

Từ khóa: *Asenat; vỏ sò biến tính photphat; hấp phụ; động học và đẳng nhiệt hấp phụ; khả năng tái sử dụng.*

Eco-friendly utilization of phosphate-modified oyster shell for efficient arsenic adsorption

ABSTRACT

Arsenic contamination in aquatic systems, especially from acid mine drainage, poses severe environmental and health risks due to the toxicity and mobility of arsenate (As(V)). In this study, oyster shell waste was valorized into phosphate-modified oyster shells (PMOS) as an eco-friendly and low-cost adsorbent for As(V) removal. PMOS was prepared through thermochemical treatment followed by phosphate functionalization, and its adsorption behavior was systematically investigated under different conditions. The results showed that As(V) removal efficiency strongly depended on pH, contact time, initial concentration, and adsorbent dosage, with optimal performance (~95% removal) achieved at pH 3 ÷ 7, a dosage of 1.0 ÷ 1.5 g/L, and equilibrium reached within 100 min. Kinetic analysis confirmed that the process followed a pseudo-second-order model, indicating chemisorption as the dominant mechanism, while isotherm studies revealed the Freundlich model provided the best fit, with a maximum adsorption capacity (qmax) of 46.34 mg/g. Structural characterization confirmed the successful incorporation of phosphate groups, enhancing affinity for arsenate through electrostatic attraction, ion exchange, and surface complexation. Importantly, reusability tests demonstrated that PMOS maintained more than 80% of its removal efficiency even after five adsorption–desorption cycles, confirming its regeneration stability. These findings highlight PMOS as a promising, sustainable, and cost-effective material for arsenic remediation in acid mine drainage-impacted waters while simultaneously contributing to circular economy strategies through aquaculture waste valorization.

Keywords: Arsenate; Phosphate-modified oyster shell; Adsorption; Kinetic and Isotherm; Reusability.

1. INTRODUCTION

Arsenic contamination in aquatic systems has emerged as a critical global issue due to its extreme toxicity, persistence, and bioaccumulative character, with chronic exposure associated with severe health risks such as cancers, cardiovascular disorders, and dermatological lesions. Among arsenic species, arsenate (As(V)) predominates under oxic conditions and is of particular concern because of its high solubility and mobility in water. In mining regions, the oxidative dissolution of sulfide minerals produces acid mine drainage, an effluent characterized by low pH and high concentrations of Fe and Mn, while simultaneously releasing considerable amounts of As(V), thereby intensifying ecological hazards and human health risks [1–3]. Although strict regulations have been established - such as the World Health Organization (WHO) provisional guideline of 0.01 mg/L and the Vietnamese national standard QCVN 01-1:2024/BYT -arsenic concentrations in acid mine drainage -impacted waters often exceed these limits by several orders of magnitude, highlighting the urgent need for efficient, robust, and affordable treatment technologies [3,4]. Conventional remediation approaches, including precipitation, ion exchange, and membrane filtration, have been widely studied and applied but are often constrained by high chemical and energy demands, secondary waste generation, and limited stability under the harsh and complex chemical conditions of acid mine drainage [5].

In recent years, the development of eco-friendly, low-cost, and sustainable adsorbents has become an essential research direction. Biomass wastes, particularly shellfish residues such as oyster shells, have attracted attention owing to their abundance, low cost, and high calcium carbonate content [6–9]. Transforming such residues into water treatment materials offers a dual environmental benefit: reducing aquaculture-derived waste and providing a renewable adsorbent for pollutant removal, in line with circular economy principles. Previous studies have demonstrated the potential of oyster shells and related derivatives for capturing heavy metals such as Pb(II), Cd(II), and Hg(II) [8,9]. However, their direct application to As(V) removal remains limited due to the scarcity of active binding sites and insufficient surface reactivity. To overcome these drawbacks, surface modification has been explored, with phosphate functionalization emerging as a highly effective strategy as recently demonstrated in several biosorbent studies published [6,10]. By introducing phosphate groups onto calcium-rich matrices, active functional sites are created that enhance electrostatic interactions, ion exchange, surface complexation, and even co-precipitation with arsenate ions [11,12]. This approach significantly improves the removal efficiency of arsenic compared to unmodified shells and provides a

sustainable pathway for waste valorization in water treatment.

Despite these advances, the application of phosphate-modified oyster shells (PMOS) to arsenic remediation in acid mine drainage -related contexts remains underexplored. This knowledge gap is crucial, since acid mine drainage presents one of the most demanding scenarios for treatment technologies due to its extreme acidity and the presence of competing metal ions. Addressing this challenge, the present study aims to transform oyster shell waste into a phosphate-modified adsorbent and evaluate its potential for efficient As(V) removal. Specifically, the work pursues three objectives: (i) to investigate the adsorption behavior of As(V) under varying conditions and optimize operational parameters, (ii) to elucidate the adsorption mechanisms through kinetic and isotherm modeling, and (iii) to assess the regeneration and reusability of PMOS across multiple cycles to determine its long-term stability. By simultaneously addressing the urgent environmental challenge of arsenic pollution in acid mine drainage -impacted waters and the sustainable valorization of aquaculture waste, this research provides both a practical solution for water treatment and a contribution to eco-friendly resource utilization.

2. EXPERIMENT

2.1. Material

Raw oyster shells were collected from seafood processing waste in Quang Ninh. Analytical-grade Sodium arsenate dibasic heptahydrate ($Na_2HAsO_4.7H_2O$) was purchased. Other reagents, including hydrochloric acid (HCl), sodium hydroxide (NaOH), and phosphoric acid (H_3PO_4), were of analytical grade.

2.2. Preparation of Phosphate-modified oyster shells

The thermochemical modification of oyster shells followed the method outlined by Huong et al [13]. The collected oyster shells were thoroughly washed, dried at 105°C for 24 hours, and crushed into particles < 0.25 mm. The pretreated shells were then subjected to thermal activation in a muffle furnace at 500°C for 2 hours. Phosphate modification was performed by immersing the calcined shells in 0.5 M phosphoric acid solution at 65°C for 2 hours under agitation to induce partial phosphatization, forming a calcium phosphate-carbonate hybrid structure. The modified material was then filtered, rinsed with DI water until reaching neutral pH, dried at 90 °C for 4 hours, and stored in airtight containers. The resulting material was labeled as PMOS.

2.3. Study on As(V) adsorption

As(V) adsorption was investigated at contact times of 15, 30, 45, 60, 90 and 120 minutes, at different initial concentrations from 5 ÷ 30 mg/L, with PMOS dosage varying from 0.25 ÷ 1.5 g/L, and environmental pH adjusted to 3, 5, 7, 9 and 11. All experiments were performed at room temperature (25 ± 2 °C) under continuous stirring at 150 rpm in 50 mL of solution. After adsorption, the suspensions were filtered, and the residual As(V) concentration was determined by ICP-MS. Adsorption kinetics and adsorption isotherm models were subsequently evaluated under the same experimental conditions. To investigate the regenerative properties of PMOS, desorption was carried out using 50 mL of 0.1 M HCl for 60 minutes. Then filter, wash, and dry at 90 degrees for 4 hours. The properties of purPMOS and desPMOS were examined by FT-IR.

2.4. Equations used

The removal efficiency (R, %) of As(V) and the adsorption capacity at equilibrium (qe, mg/g) were calculated using the following equations:

$$R(\%) = \frac{C_0 - C_e}{C_0} \times 100 \quad (1)$$

$$q_e = \frac{(C_0 - C_e)V}{m} \quad (2)$$

where

C_0 (mg/L) is the initial As(V) concentration,

Ce (mg/L) is the equilibrium concentration,

V (L) is the solution volume, and

m (g) is the dry mass of the adsorbent (PMOS).

To evaluate the adsorption behavior of As(V) on PMOS, several commonly used kinetic and isotherm equations in linear form were employed. Only the mathematical expressions required for fitting are provided here.

Kinetic equations

Pseudo-first-order (PFO):

$$log(q_e - q_t) = logq_e - \frac{k_1}{2.303}t \quad (3)$$

Pseudo-second-order (PSO):

$$\frac{t}{q_t} = \frac{1}{k_2 q_e^2} + \frac{t}{q_e} \quad (4)$$

Elovich:

$$q_t = \frac{1}{\beta}\ln(\alpha\beta) + \frac{1}{\beta}lnt \quad (5)$$

Intraparticle diffusion (IPD):

$$q_t = k_i t^{1/2} + C \quad (6)$$

Bangham:

$$log\left[\log\left(\frac{C_0}{C_0 - q_t m/V}\right)\right] = \log\left(\frac{k_0 m}{2.303V}\right) + \alpha log t \quad (7)$$

where:

k_1 (min^{-1}): pseudo-first-order rate constant,

k_2 (g/mg.min): pseudo-second-order rate constant,

α (mg/g.min): initial Elovich adsorption rate,

β (g/mg): Elovich desorption coefficient,

k_0: Bangham kinetic constant,

α (dimensionless in Bangham eq.): diffusion exponent,

k_i ($mg/g.min^{0.5}$): intraparticle diffusion constant,

C: boundary layer thickness parameter.

Isotherm equations

Freundlich isotherm (multilayer, heterogeneous surface):

$$log q_e = log K_F - \frac{1}{n} log C_e \quad (8)$$

Langmuir isotherm (monolayer):

$$\frac{C_e}{q_e} = \frac{1}{K_L q_{max}} + \frac{C_e}{q_{max}} \quad (9)$$

Temkin isotherm:

$$q_e = B ln K_T + B Ln C_e \quad (10)$$

K_T ($L.mg^{-1}$): Temkin equilibrium binding constant,

B ($mg.g^{-1}$): Temkin constant related to adsorption heat .

Dubinin–Radushkevich (D–R) isotherm:

$$ln q_e = ln q_{max} - \beta \varepsilon^2 \quad (11)$$

$$\varepsilon = RT ln\left(1 + \frac{1}{C_e}\right) \quad (12)$$

Adsorption energy:

$$E = \frac{1}{\sqrt{2\beta}} \quad (13)$$

Henry isotherm:

$$q_e = K_H C_e \quad (14)$$

where:

K_L (L/mg): Langmuir constant,

q_{max} (mg/g): maximum adsorption capacity,

K_F ((mg/g)(L/mg)$^{1/n}$): Freundlich constant,

1/n: Freundlich heterogeneity factor,

K_T (L/mg): Temkin binding constant,

B (mg/g): Temkin constant proportional to adsorption heat,

β (mol²/kJ²): D–R constant related to adsorption energy,

ε: Polanyi potential,

K_H (L/mg): Henry constant.

3. RESULTS AND DISCUSSION

3.1. Study on the adsorption conditions of As(V) in water by PMOS

Figure 1 shows that the As(V) ion removal efficiency strongly depends on the environmental conditions and the dosage of PMOS adsorbent. In graph (a), the adsorption efficiency reaches the highest value (~97.5%) at pH = 2 ÷ 4 and gradually decreases as the pH increases, especially at alkaline pH (>10). This phenomenon can be explained through two key factors: (i) the chemical transformation of As(V) with pH and (ii) the surface charge state of PMOS (pHpzc = 8.054). The pHpzc value of PMOS was determined using the pH drift method, in which the adsorbent was added to a series of 0.01 M NaCl electrolyte solutions with initial pH values adjusted from 2 to 12 and allowed to equilibrate for 24 hours.

At low pH, the main form is $H_2AsO_4^-$; when pH increases to neutral and slightly alkaline, $HAsO_4^{2-}$ predominates; and in strong alkaline environments, AsO_4^{3-} becomes the main form. On the material side, pHpzc = 8.054. When pH < pHpzc, the PMOS surface carries a positive charge, which is favorable for electrostatic attraction of arsenate anions. On the contrary, at pH > pHpzc, the surface turns negatively charged, causing electrostatic repulsion of anions and and simultaneously competes with OH- in the solution. Therefore, in acidic environments (3 < pH < 7), when As(V) mainly exists in the form of $HAsO_4^{2-}$ and the material surface is positively charged, the adsorption mechanism occurs strongly thanks to the combination of electrostatic interactions and ion exchange at the active phosphate groups on the brushite structure ($CaHPO_4 \cdot 2H_2O$). Graph (b) shows that the adsorption rate of As(V) is fast, with an efficiency of over 80% after only 45 min and almost saturated (~95%) after 100 ÷ 120 min. This reflects the adsorption mechanism that combines surface interaction and intraparticle diffusion, and demonstrates that PMOS has the ability to process quickly and efficiently.

In graph (c), the efficiency decreases as the initial As(V) concentration increases. At low concentrations (5 ÷ 10 mg/L), the efficiency reaches over 94 ÷ 95%, but drops to about 90% when the concentration increases to 30 mg/L. The reason is that the number of adsorption sites is limited, when the pollutant concentration is too high, the material is saturated and the efficiency decreases.

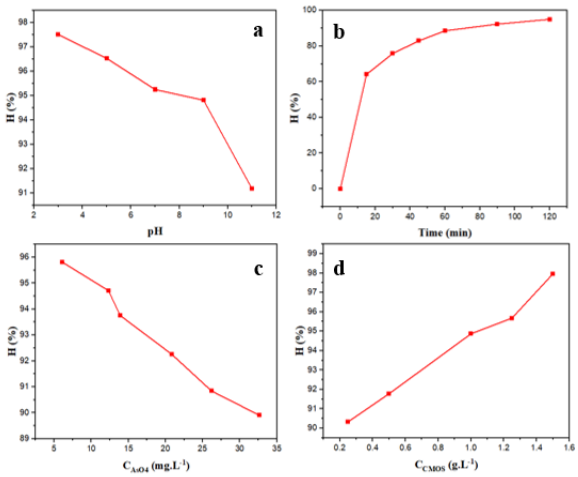

Figure 1. Graph of As(V) treatment efficiency at different environmental pH (a), time (b), As(V) concentration (c), PMOS dosage (d).

3.2. Kinetic model and As(V) adsorption isotherm

Based on Figure 2 and the data in Table 1, it can be seen that the adsorption process of As(V) on PMOS materials is best described by the pseudo-second-order kinetic model, with a correlation coefficient R^2 of 0.9997 and a qe value (11.78 mg/g) that closely matches the experiment. This shows that the main mechanism of the process is chemisorption, in which the active hydroxyl and phosphate groups on the material surface play a central role, creating a strong interaction with arsenate ions. Meanwhile, the pseudo-first-order model also shows a certain level of agreement (R^2 = 0.9742) but the qe value is significantly different, indicating that it does not accurately reflect the actual kinetics. The Elovich model (R^2 = 0.9839) adds further evidence of the energy heterogeneity at the adsorption sites, indicating that the PMOS surface contains many active sites with different properties. In particular, the bangham model has a very high R^2 (0.9968), confirming the significant role of capillary diffusion in controlling the adsorption rate. In contrast, the intraparticle diffusion model with R^2 of only 0.7710 shows that intraparticle diffusion is not the decisive step but only contributes to support. Observation of the time survey curve (Figure 2f) shows that the adsorption rate is fast in the initial stage, the efficiency reaches more than 80% after only 45 minutes and approaches equilibrium at about 100 minutes with an efficiency of nearly 95%. This evolution reflects a multi-stage adsorption mechanism: initially, the rapid capture of As(V) ions on the surface, followed by a slow diffusion process into the pores inside the material.

Thus, combining the data in Figure 2 and Table 1, it can be confirmed that the adsorption kinetics of As(V) on PMOS follows a pseudo-second-order model, which is typical for chemical adsorption, and is supported by the diffusion mechanism in the capillary. This is an important factor that helps the material achieve fast processing speed, high efficiency and potential for practical application in the treatment of arsenic in water.

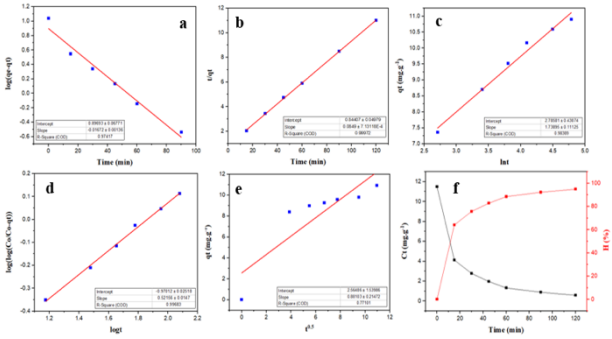

Figure 2. Kinetic model of As(V) adsorption by PMOS according to first-order kinetics (a), second-order kinetics (b), Elovich (c), Bangham (d), intrapartical diffusion (e), and time study (f) of the process.

Table 1. Parameters of As(V) adsorption kinetic models on phosphate-modified oyster shells (PMOS)

Kinetic model	Parameter	Value
Pseudo-first order	k_1 (min^{-1})	0.0385
	q_e (mg/g)	7.8873
	R^2	0.9742
Pseudo-second order	k_2 (g/mg.min)	0.0085
	q_e (mg/g)	11.7786
	R^2	0.9997
Elovich	a (mg/g)	2.7858
	b (g/mg)	1.7390
	R^2	0.9839
Bangham	α	0.157
	log(k_om / 2.303V)	-0.9701
	R^2	0.9968
Intrapartical diffusion	k_i (mg/g.min$^{0.5}$)	0.8810
	C (mg/g)	2.5649
	R^2	0.7710

Based on Figure 3 and the data shown in Table 2, it can be seen that the adsorption process of As(V) on PMOS materials is best described by the Freundlich isotherm model, with a correlation coefficient R^2 of 0.9868, higher than other models. This shows that the PMOS surface is heterogeneous, there are many adsorption sites with different energies, and the adsorption process occurs according to a multilayer mechanism. The value of n = 1.56 > 1 also proves the favorable and good adsorption capacity of the material for As(V). The Langmuir model also gives a relatively good fit (R^2 = 0.9803), with a maximum adsorption capacity qmax = 46.34 mg/g, reflecting the ability to form a monomolecular coating on the material surface. This qmax value is significantly higher than that of many other biological materials, demonstrating the outstanding advantage of PMOS in arsenic treatment. The Temkin model (R^2 = 0.9650) shows that the adsorption energy gradually decreases as the surface coverage increases, consistent with the characteristics of materials rich in active phosphate groups.

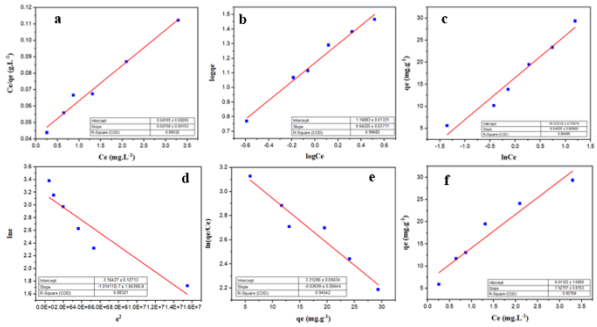

Figure 3. PMOS adsorption isotherm models of As(V) according to Langmuir (a), Freundlich (b), Temkin (c), Dubinin–Radushkevich (d), Elovich (e), Henry (f).

Table 2. Parameters of isotherm models for As(V) adsorption on phosphate-modified oyster shell (PMOS)

Isothermal model	Parameter	Value
Langmuir	K_L (L/mg)	0.518
	q_{max} (mg/g)	46.34
	R^2	0.9803
Freundlich	K_F (mg/g).(L/mg)$^{1/n}$	14.75
	n	1.56
	R^2	0.9868
Temkin	K_T	5.657
	b_T (J/mol)	9.540
	R^2	0.9650
Dubinin-Radushkevich	β (mol^2/kJ^2)	1.0141.10^{-7}
	E (kJ/mol)	2220.46
	R^2	0.8832
Elovich	α (mg/g)	27.463
	β (g/mg)	0.0370
	R^2	0.9454
Henry	K_H	7.5276
	R^2	0.9377

In contrast, the Dubinin–Radushkevich model (R^2 = 0.8832) gives a qmax value of only 23.67mg/g, much lower than Langmuir model, while the adsorption energy (E) reaches 2.22 kJ/mol, which is typical of physical adsorption. Although the Elovich (R^2 = 0.9454) and Henry (R^2 = 0.9377) models have quite good correlation coefficients, they do not fully reflect the kinetic nature and complex interaction mechanism between As(V) and the material surface.

Thus, it can be concluded that the Freundlich model is the most suitable to describe the adsorption process of As(V) on PMOS, indicating the existence of a multilayer mechanism on a heterogeneous surface, while the Langmuir model still provides important information on the maximum capacity with qmax reaching 46.34 mg/g, confirming the high efficiency and application potential of the material in the treatment of arsenic-contaminated water.

The results in Table 3 show that the phosphate-modified oyster shell material (PMOS) achieved a maximum adsorption capacity of qmax = 46.34 mg/g for As(V), confirming its remarkable arsenate removal efficiency. Compared with natural and simply modified mineral materials, PMOS showed outstanding advantages. Specifically, the qmax value of PMOS was several times higher than that of the kaolin mixture system (0.695 ÷ 4.17 mg/g) [14], and nearly three times higher than that of ascorbic acid-coated Fe_3O_4 magnetic nanoparticles (16.56 mg/g) [4]. At the same time, PMOS also surpasses other As(V) removal materials such as NaOH-modified electrolytic manganese sludge (23.96 mg/g) [15], iron-modified concrete sludge (27.8 ÷ 41.7 mg/g) [16], or GUT-3 metal-organic framework (33.91 mg/g). This demonstrates that the phosphate modification process significantly optimized the surface activity of oyster shells, helping to increase the density of phosphate and hydroxyl functional groups, thereby enhancing the ability to capture arsenate anions. In addition, when compared with more advanced material systems, PMOS continues to maintain its competitive position. The adsorption capacity of PMOS is higher than that of the metal–organic framework –

chitosan – nanocellulose (CS-NC-MIL-53(Fe)) (36.76 mg/g) [17], and only lower than some materials with more complex structures such as the polymer–Fe–Al hydroxide hybrid (49.6 mg/g) [18] or amine-modified lignin (64.08 mg/g) [19]. This shows that PMOS, although developed from simple biological waste sources, can still achieve adsorption efficiency approaching or even surpassing some modern nano-composite materials which have complex manufacturing processes, high costs and are difficult to apply on a large scale.

Table 3. Comparison of maximum adsorption capacity (qmax) of PMOS and As(V) adsorbent tracks.

Adsorbent material	q_{max} (mg/g)	References
Kaolin mixed system	0.695 ÷ 4.17	[14]
Ascorbic Acid Coated Superparamagnetic Fe_3O_4 Magnetic Nanoparticles	16.56	[4]
NaOH modified electrolytic manganese residues (M-EMRs)	23.96	[15]
Waste sludge from the production of iron-modified concrete (CWSFe)	27.8 ÷ 41.7	[16]
Metal-organic framework – chitosan - nanocellulose (CS-NC-MIL-53(Fe))	36.76	[17]
GUT-3 metal organic framework	33.91	[12]
Phosphate - modified oyster shell	46.34	This study
Polymer-Fe-Al hydroxide hybrid material	49.6	[18]
Amine-modified lignin (Lignin@N-X)	64.08	[19]

3.3. Reuse of PMOS in As(V) adsorption

Figure 4 shows the FT-IR graphs of PMOS before adsorption (purPMOS) and after desorption (desPMOS). The PMOS sample before adsorption (purPMOS) exhibits the inherent absorption bands of $CaCO_3$, and the PMOS FT-IR spectrum shows many important new signals. The broad peaks at 3479 and 3160 cm^{-1} reflect the O–H stretching vibrations, indicating the presence of hydroxyl groups or adsorbed water. The peak at 1646 cm^{-1} is assigned to the bending vibration of H–O–H, further confirming the existence of water molecules in the newly formed structure. In particular, a series of bands at 1416, 1123, 1056 and 984 cm^{-1} are characteristic of the valence and deformation vibrations of the phosphate group (PO_4^{3-}/HPO_4^{2-}) [20]. In addition, the peak at 522 cm^{-1} is attributed to the Ca–O and P–O bond vibrations in the calcium phosphate salt structure. The appearance of these peaks shows that the denaturation process was successful in introducing phosphate groups into the $CaCO_3$ matrix, while forming the $CaHPO_4{\cdot}2H_2O$ (Brushite) phase [21].

It can be seen that after desorption with 0,1 M HCl (desPMOS), most of the main peaks were restored to almost the original spectrum, especially –OH and CO_3^{2-}, indicating that the Ca^{2+}– PO_4^{3-} - CO_3^{2-} framework structure of the material is still stable. However, the intensity of the clusters at 1123.09 ÷ 1056.19 cm^{-1} and 522.64 cm^{-1} remain lower than the original spectrum, indicating that part of the metal ions are still firmly bound in the form of stable phosphate or carbonate species, which are difficult to remove completely. This confirms that the adsorption mechanism of PMOS is based on the coordination between ion exchange, surface precipitation and strong chemical bonding, and the material has good regeneration ability after desorption.

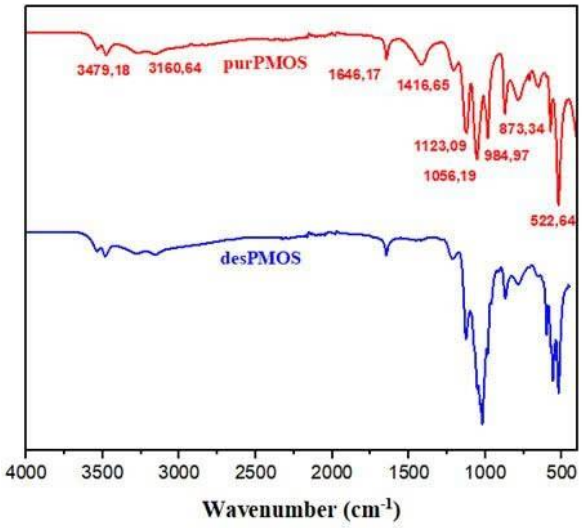

Figure 4. FT-IR graphs of the material before adsorption (purPMOS), and after desorption (desPMOS).

The results of the reusability evaluation (Figure 5) showed that PMOS exhibited stable and sustainable regeneration in the process of As(V) removal. In the first cycle, the adsorption efficiency reached 94.96%, reflecting the very high ability of the material to capture As(V) ions. During desorption and reuse, the efficiency slightly decreased but remained high through the

following cycles, with a value of over 90% in the second cycle, about 88 ÷ 89% in the third cycle, and still reaching about 84% and 81% after the fourth and fifth cycles. This decrease is inevitable because a part of As(V) ions are tightly held at adsorption sites with high binding energy or due to local changes on the material surface after many treatments, however, the level of decrease is quite small compared to the total initial efficiency. It is noteworthy that the decreasing trend occurred gradually rather than abruptly, clearly reflecting the structural stability and the ability to preserve the active functional groups of PMOS during the repeated adsorption-desorption process. This shows that most of the active sites can still be effectively reactivated after the desorption process, and proves that the material is not destroyed or deactivated as quickly as many traditional adsorbents. Maintaining the As(V) removal efficiency above 80% even after 5 consecutive reuse cycles confirms that PMOS is a material with good regenerability, high durability and promise for practical implementation. With this characteristic, PMOS not only meets the requirements for treatment efficiency but also brings great economic and sustainability advantages, because the ability to regenerate many times will reduce operating costs, limit the need to replace new materials, and reduce the amount of solid waste generated during the water treatment process. Thus, the adsorption capacity combined with sustainable regeneration makes PMOS a promising adsorption candidate for As(V) removal in aquatic environments, serving long-term, safe and effective treatment solutions.

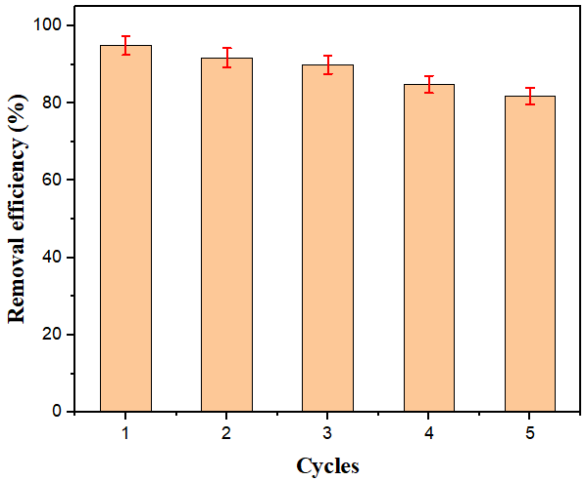

Figure 5. Reusability of PMOS for As(V) adsorption.

4. CONCLUSION

In this study, a phosphate-modified oyster shell (PMOS) adsorbent was successfully developed and systematically evaluated for As(V) removal from aqueous environments. The novelty of this work lies in: (i) introducing phosphate groups onto a naturally calcium-rich biomaterial to create new, highly reactive As(V) binding sites; (ii) converting low-value aquaculture waste into an efficient functional adsorbent; and (iii) demonstrating high adsorption performance under acidic conditions that are characteristic of acid mine drainage - an application scenario rarely addressed for biosorbent-based materials.

PMOS exhibited outstanding removal efficiency (~95%) under optimal conditions (pH 3 ÷ 7, dosage 1.0 ÷ 1.5 g/L, equilibrium time ~100 min). The adsorption followed a pseudo-second-order kinetic model, suggesting chemisorption dominated by surface interaction with phosphate–calcium active centers, while Freundlich isotherm fitting confirmed multilayer adsorption on heterogeneous surfaces. The material achieved a high maximum adsorption capacity (qmax = 46.34 mg/g), which surpasses many previously reported biosorbents and highlights the enhanced reactivity generated by phosphate modification.

Structural analysis verified the successful incorporation of phosphate functionalities, which played a decisive role in strengthening the affinity toward arsenate oxyanions. Furthermore, regeneration experiments demonstrated that PMOS maintained over 80% of its adsorption efficiency after five reuse cycles, confirming the stability of its modified framework and its practical suitability for long-term operation.

Overall, the present study not only clarifies the adsorption mechanisms of As(V) on phosphate-modified calcium biomaterials but also provides a sustainable, low-cost, and scalable solution for arsenic removal in acidic mining-impacted waters. By integrating waste valorization with high-performance water treatment, this work contributes a new material concept and practical pathway aligned with circular-economy strategies and environmentally responsible remediation technologies.

Acknowledgments

REFERENCES

1. D. Núñez-Gómez, F. R. Lapolli, M. E. Nagel-Hassemer, M. Á. Lobo-Recio. Optimization of Fe and Mn removal from coal acid mine drainage (AMD) with waste biomaterials: Statistical modeling and kinetic study, *Waste and Biomass Valorization*, **2020**, *11(3)*, 1143–1157.
2. T. T. Nguyen, H. Huang, T. A. H. Nguyen, S. Soda. Recycling clamshell as substrate in lab-scale constructed wetlands for heavy metal

removal from simulated acid mine drainage, *Process Safety and Environmental Protection*, **2022**, *165*, 950–958.
3. K. Khan, et al. Pathways and risk analysis of arsenic and heavy metal pollution in riverine water: Application of multivariate statistics and USEPA-recommended risk assessment models, *Journal of Contaminant Hydrology*, **2025**, *269*, 104483.
4. X. Huang, Y. Liu, X. Wang, L. Zeng, T. Xiao, D. Luo, J. Jiang, H. Zhang, Y. Huang, M. Ye, L. Huang. Removal of arsenic from wastewater by using nano Fe_3O_4/Zinc organic frameworks, *International Journal of Environmental Research and Public Health*, **2022**, *19(17)*, 10897.
5. M. Yadav, G. Singh, R. N. Jadeja. Physical and chemical methods for heavy metal removal, *Pollutants and Water Management: Resources, Strategies and Scarcity*, **2021**, 377–397.
6. Z. Zhou, Y. Wang, S. Sun, Y. Wang, L. Xu. Preparation of PVA/waste oyster shell powder composite as an efficient adsorbent of heavy metals from wastewater, *Heliyon*, **2022**, *8(12)*, e12014.
7. H. Qin, T. Hu, Y. Zhai, N. Lu, J. Aliyeva. The improved methods of heavy metals removal by biosorbents: A review, *Environmental Pollution*, **2020**, *258*, 113777.
8. G. Zhao, X. Wang, Q. Chen, J. Cheng. Efficacy of phosphorus loaded oyster shell in heavy metal removal: A combined study on adsorption behavior, structure characterization and comparative mechanism, *Environmental Technology & Innovation*, **2024**, *33*, 103484.
9. T.-T. Tran, N.-N. T. Tran, S. Sugiyama, J.-C. Liu. Enhanced phosphate removal by thermally pretreated waste oyster shells, *Journal of Material Cycles and Waste Management*, **2021**, *23*(1), 177–185.
10. G. Zhao, X. Wang, Q. Chen, J. Cheng. Efficacy of phosphorus loaded oyster shell in heavy metal removal: A combined study on adsorption behavior, structure characterization and comparative mechanism, *Environmental Technology & Innovation*, **2024**, *33*, 103484
11. P. Keerthana Devi, A. Geethakarthi. Arsenic removal using calcium hydroxyapatite synthesized from paper mill sludge, *Applied Water Science*, **2022**, *12(8)*, 174.
12. X. Zheng, et al. Efficient removal of As(V) from simulated arsenic-contaminated wastewater via a novel metal–organic framework material: Synthesis, structure, and response surface methodology, *Applied Organometallic Chemistry*, **2020**, *34*(5), e5584.
13. T. T. H. Nguyen, et al. Biomass conversion of waste oyster shells into calcium phosphate/carbonate adsorbents for efficient manganese removal, *Biofuels, Bioproducts and Biorefining*, **2025,** *19.4*, 1044-1058.
14. B. Doušová, et al. Kaolin–fly ash composite for Pb^{2+} and AsO_4^{3-} adsorption from aqueous system, *Applied Sciences*, **2024**, *14*(12), 5358.
15. J. Lan, et al. Highly efficient removal of As(V) with modified electrolytic manganese residues (M-EMRs) as a novel adsorbent, *Journal of Alloys and Compounds*, **2019**, *811*, 151973.
16. B. Doušová, et al. Adsorption properties of waste building sludge for environmental protection, *Minerals*, **2021**, *11*, 309.
17. Y. Paisart. Nanocellulose-chitosan-metal organic framework composites for arsenic removal, *Journal of Environmental Chemical Engineering*, **2021**, *9*(5), 106075.
18. P. S. Kumar, R. Q. Flores, C. Sjöstedt, L. Önnby. Arsenic adsorption by iron–aluminium hydroxide coated onto macroporous supports: Insights from X-ray absorption spectroscopy and comparison with granular ferric hydroxides, *Journal of Hazardous Materials*, **2016**, *302*, 166–174.
19. Q. Wu, et al. Aminated lignin by ultrasonic method with enhanced arsenic(V) adsorption from polluted water, *Advanced Composites and Hybrid Materials*, **2022**, *5*(2), 1044–1053.
20. M. P. Hofmann, A. M. Young, U. Gbureck, S. N. Nazhat, J. E. Barralet. FTIR-monitoring of a fast setting brushite bone cement: effect of intermediate phases, *Journal of Materials Chemistry*, **2006**, *16*, 3199–3206.
21. P. M. Nkebiwe, K. Sowoidnich, M. Maiwald, B. Sumpf, T. E. Hartmann, D. Wanke, T. Müller. Detection of calcium phosphate species in soil by confocal μ-Raman spectroscopy, *Journal of Plant Nutrition and Soil Science*, **2022**, *185(2)*, 221–231.